5

Mixing and Segregation

Thorough mixing of particles in the transverse plane of a rotary kiln is fundamental to the uniform heating or cooling of the charge and, ultimately, to the generation of a homogeneous product. However, differences in particle size and density result in a de-mixing process whereby smaller or denser particles segregate to form an inner core or kidney of segregated material which may never reach the bed surface to be exposed to freeboard temperatures. In this chapter an analytical model and its numerical solution is developed which relates particle segregation rates to primary operating parameters such as rotary kiln diameter, bed depth, and rotational speed. The model considers a binary mixture of small and large particles in the continuously shearing active region of the kiln bed. Continuum equations are employed to describe the mixing and segregation rates in the transverse plane of the bed that result from both particle percolation and diffusional mixing. The granular flow model developed in Chapter 4 provides the flow field needed for the convective terms for material concentration and the diffusion coefficients. The percolation velocities are generated using existing models that relate percolation to the probability of void formation in the shear plane.

The rheological properties of the bed material can be expected to change during the passage of a charge through a rotary kiln. Severe changes can result in alterations to material properties, such as particle size, shape, surface character, and these ultimately may result in

distinct changes to bed behavior. One such behavioral phenomenon is segregation which, since it acts as a mechanism of de-mixing, may influence heat transfer within the bed. Segregation may also influence the rate at which particles are elutriated from the exposed bed surface when, for example, large amounts of gas are being released from the bed. Additionally, the effect of segregation on heat transfer is of considerable practical importance since it may significantly influence the degree of product homogeneity.

The main causes of segregation are differences in particle size, density, shape, roughness, and resilience (Williams and Khan, 1973). Although any of these may produce segregation under certain circumstances, most rotary kiln segregation issues arise from differences in particle size (Pollard and Henein, 1989) and the work described herein is focused on this phenomenon. The mechanisms by which size segregation occurs might be classified as trajectory segregation or percolation (Williams and Khan, 1973; Bridgwater et al., 1985).

1. Trajectory segregation: This is due to the fact that, for certain modes of kiln operation, particles being discharged from the plug flow region into the active layer may be projected horizontally from the apex onto the exposed bed surface. This situation may apply in the slumping, rolling, and cataracting modes, whereby different sized particles are emptied onto the surface during material turnaround. It has been suggested that the distance over which these particles travel is proportional to the square of the particle diameter (Bridgwater, 1976), which means that finer particles will tend to be concentrated at the mid-chord section.
2. Percolation: When a bed of particles is disturbed so that rearrangement takes place (rapid shearing), the probability that a particle will find a void into which to fall depends on the size of the particles (Savage, 1983). Thus smaller particles will tend to filter downward through a bed of flowing granular material while large particles will simultaneously tend to be displaced upward.

Trajectory segregation has been identified (Bridgwater et al., 1985) as the main cause of axial segregation or "banding" whereby particles of different sizes are selectively collected into bands occurring over the kiln length. This axial segregation is not considered in the present work and therefore not critically reviewed; rather, attention

is focused on segregation in the transverse plane, specifically, percolation. Although percolation theory, also known as inverse sieving in granular flow models (Savage, 1989), is reasonably well developed, it has seldom been employed to model segregation patterns encountered in rotary kilns. Instead, most of the rotary kiln literature characterizes the rate of segregation by a first or second order type kinetic expression such as Nityanand et al., 1986; Pollard and Henein, 1989

$$S_n = A \times (Fr)^b \tag{5.1}$$

where S_n is defined as the normalized rate of segregation, Fr is the rotational Froude number, and A and b are experimentally determined kinetic parameters.

Size segregation in failure zones, for example, the active (shearing) region of a rolling bed in a rotary kiln or gravity flow on an incline (also known as free surface segregation), has been described by the mechanism of percolation (Bridgwater et al., 1985; Savage, 1989). Size segregation in such systems is considered as a random continuous network whereby voids are randomly formed and distributed (Figure 5.1).

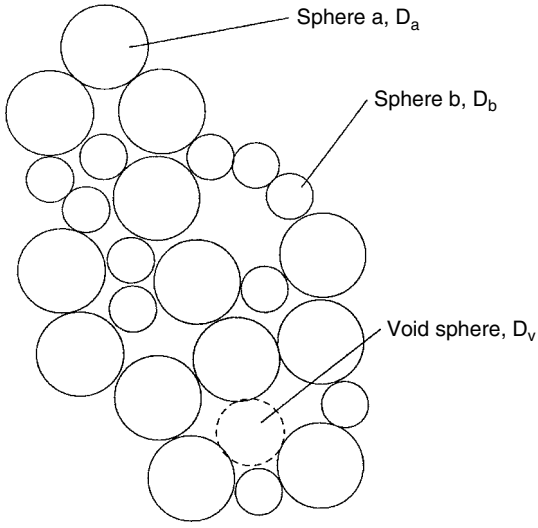

Figure 5.1 Random continuous network of segregating particles (Savage, 1989).

For gravity flow on an incline Savage and Lun (1988) approached the problem by considering three events:

1. The probability of voids forming that are of sufficient size for the smaller particles to percolate into. The probability of such voids forming has been given as

$$p(E) = \frac{1}{\overline{E} - E_m} \exp\left\{\frac{E - E_m}{\overline{E} - E_m}\right\} \tag{5.2}$$

   where E is the void diameter ratio which is defined as the ratio of the void diameter to the average void diameter, that is, $E = (D_v/\overline{D})$. E_m is the minimum possible void diameter ratio and $\overline{E}$ is the mean void diameter ratio. $E_m = 0.154$ is the value for which voids in a packing will result in spontaneous percolation (Bridgwater et al., 1971).

2. The capture of particles by voids in the underlying layer. For this event the number of particles captured by a void per unit time is dependent on the velocity differences between two neighboring shear layers.

3. The establishment of a mass flux of small particles. When this occurs the average percolation velocities in the plane normal to the bed surface can be determined by material balance.

The proposed sequence of events is useful in exploring the possibility of employing the physically derived continuum equations required to solve for the concentration gradients with a minimum probabilistic input. The stochastic approach tends to conceal the detailed behavior and the mechanisms that are the source of industrial problems (Bridgwater, 1976). This may also be said about the characterization of segregation by degree of mixing or by kinetic expressions such as the one given in Equation (5.1). Such expressions will conceal all the interparticle mechanisms in a single parameter that serves little or no industrial purpose.

Although classification as applied to solids is synonymous with different sizes of the same material it should be pointed out that other classifications, such as particle density or mass, and even particle shape, can also cause mixing or segregation. It has recently been established (Alonso et al., 1992) that size and density differences can, indeed, be combined to reduce segregation through mutual compensation.

5.1 Modeling of Particle Mixing and Segregation in Rotary Kilns

It is evident from operator experience that thorough mixing of particles in the transverse plane of a rotary kiln is fundamental to achieving uniform heating or cooling of the charge and, ultimately, to the production of a homogeneous product. This is particularly so for processes involving granular materials. In the modeling of granular flows one generally assumes that particles are evenly sized and that mixing effectively means that (statistically) exposure to freeboard will be the same for all particles. Unfortunately, when significant variation in particle sizing occurs, there will be the tendency of small particles in the active layer to sieve downward through the matrix of larger particles. Therefore, the bed motion presented in Chapter 4 tends to concentrate finer material within the core (Figure 5.2). Material within the core, because it has very little chance of reaching the exposed bed surface for direct heat transfer from the freeboard, tends to be at a lower temperature than the surrounding material. Thus segregation can counteract advective transport of energy and thus can promote temperature gradients within the bed. However, the net effect might not necessarily be negative because for a process such as limestone calcination where smaller particles react faster than larger ones (at the same temperature), segregation of fines to the cooler core may be essential to obtaining uniform calcination of all particles. This suggests that particle size

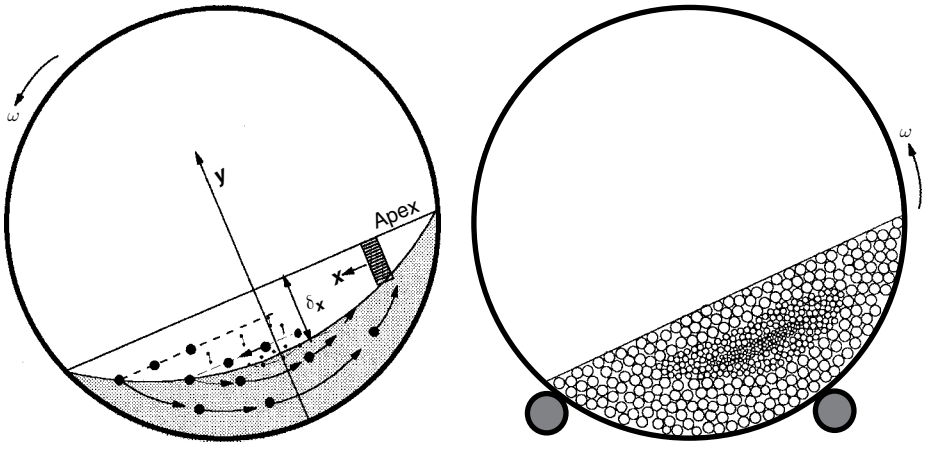

Figure 5.2 Segregated core at the cross section of a rotary calciner.

distribution in the feed material might be optimized, if our predictive capabilities for determining material mixing and segregation were well developed.

With an adequate granular flow model, a logical extension is to construct a mathematical model that will describe the phenomenon of segregation and predict the extent and dimensions of the segregated core which has become an integral part of processing real materials in rotary kilns. It is not fair to say that the modeling of segregation has not been addressed because it is a well known phenomenon in applications such as rotary mixers and has been characterized in many ways. Fan and Wang (1975) reviewed over 30 forms of mixing indices that have appeared in the literature to characterize particulate mixing and segregation in drum mixers. However, most of these characterization parameters are probabilistic or statistical in nature and, although often helpful, tend to conceal the details of the phenomenon and yield little information on, for example, the effect of material properties on flow and hence on segregation. Scaling factors are also difficult to evaluate without a good grasp of the physical phenomena that drive segregation.

We will consider a segregation model composed of a binary mixture of small and large particles in the continuously shearing active layer of the kiln bed. We will employ continuum equations to describe the mixing and segregation rates in the transverse plane of the bed that result from both particle percolation and diffusional mixing. The diffusion coefficients and the convective terms for material concentration in the continuum equations can be obtained from the granular flow model in Chapter 4. Percolation velocities are calculated along with void formation in the shear plane (Savage, 1988). Finally, the developed segregation model is applied in order to predict the size and extent of the segregated core as well as to show the effect of segregation on material mixing and on the effective thermal conductivity of the bed.

5.2 Bed Segregation Model

The mechanism of segregation as observed in rotary kilns indicates that percolation is the primary cause of driving smaller size particles to the core of the bed. To model the phenomenon, several

sequential processes must be used, including the following observed conclusions about the phenomenon:

1. From a condition of uniform mixing of particles within the bed, radial segregation proceeds very rapidly and is fully implemented within 2 to 10 kiln revolutions (Rogers and Clements, 1971; Pollard and Henein, 1989). The mechanism of segregation can therefore be considered as a steady-state problem.
2. The segregation process is continuous and there is a constant discharge of fines from the plug flow region into the active layer. This discharge of fines occurs in the upper part of the bed toward the apex and is followed by percolation normal to the bed surface as material is sheared in the active layer.
3. The resultant segregated core, popularly known in the industry as the "kidney" (or "tongue") does not consist entirely of fine particles but also contains a small amount of coarse particles (i.e., there are concentration gradients even in the core).
4. The bulk velocity distribution in the active layer does not change with addition of fines and the bed behavior (e.g., rolling, slumping, etc.) remains unchanged with fines (Henein, 1980).
5. The percolation velocity of fine particles depends on the size of the voids formed in an underlying layer; these voids are formed in a random manner (Savage, 1988).
6. For particles below some critical size, spontaneous percolation may also occur in the plug flow region thereby resulting in a possible collection of fines near the bed/wall interface (Bridgwater and Ingram, 1971).
7. Downward movement of segregating particles in the active layer is compensated by an equal volumetric upward movement of bulk particles in the active layer in a phenomenon known as "squeeze expulsion mechanism", Savage, 1988).

Based on this information a credible mathematical model can be constructed. We consider a control volume in the active layer that accounts for the mass conservation of the sinking and/or floating particles. We restrict the analysis to the active layer because, in view of (6) above, the probability of fines moving through the plug flow

region is very low compared to the dilated shearing flow in the active layer. The plug flow region can therefore be assumed to be impermeable. It serves only as the circulation path by which particles are fed back to the active layer. This assumption therefore precludes spontaneous percolation from the model. The situation to model is shown schematically in Figure 5.3a and Figure 5.3b. For convenience, the coordinate system used here is consistent with that in the flow model where a Cartesian system is allocated to the active layer such that $0 \le x \le 2L$ where $2L$ is the chord length, and the origin is at the apex of the bed.

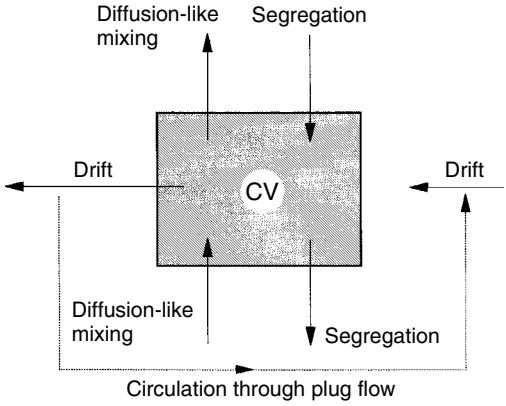

Figure 5.3a Control volume for material conservation in the active layer.

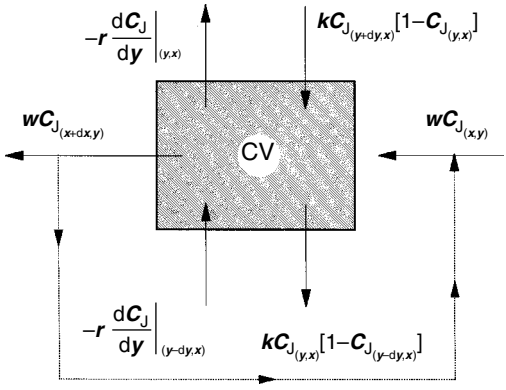

Figure 5.3b Mathematical description for material balance in control volume; the convective flux.

We consider a simple binary system of two particle sizes, each of the same density in the control volume. Since the calculation domain is restricted to the active layer, the fine particles are assumed to be larger than the critical size that causes spontaneous percolation. The situation occurs when the diameter ratio of the small to large particles exceeds the critical value, which, for a closely packed bed, has been given as (Savage, 1988)

$$\overline{\sigma} = \frac{d_{ps}}{d_{pL}} \leq 0.1547 \tag{5.3}$$

where d_{ps} and d_{pL} are, respectively, the sizes of the small and large particles for the binary system. By choosing the size ratio to be greater than the critical value it is implicitly assumed that percolation will occur only when the voids formed are larger than the smaller size particle, d_{ps}, of the binary mixture. For the active layer of the rotary kiln where continuous shearing is occurring, it will be further assumed that void formation is a random occurrence and follows a probability law. For generality we assign the term "jetsam" to sinking particles, either due to size or density differences, and "flotsam" to floating particles which the fines displace (Gibilaro and Rowe, 1974). The model is derived on a volume balance basis and the concentration terms refer to volumetric fraction of jetsam in a given volume of solids. The relationship between the volume fraction jetsam concentration and the number of particles in the control volume can, therefore, be expressed as

$$C_J = \nu \frac{\overline{\eta}\,\overline{\sigma}^3}{1 + \overline{\eta}\,\overline{\sigma}^3} \tag{5.4}$$

where ν is the solids concentration, $\overline{\eta}$ is the particle number ratio, n_J/n_F, with n_J and n_F being the respective jetsam and flotsam number particles. This relation is developed in Appendix 5A for jetsam loading of the kiln.

Following on with the continuum assumption, the control volume required for the material balance is shown in Figure 5.3a. The equilibrium concentration of jetsam within the control volume depends on the interaction of three components: (i) convection (drift) caused by the bulk velocity, (ii) diffusion-like mixing, and (iii) segregation associated with movement through voids. The rate at which jetsam is spread over the cross section is mathematically depicted in Figure 5.3b. Of the three mechanisms shown, segregation is the only one that

distinguishes jetsam from flotsam and it depends on the percolation of jetsam into the underlying layer and subsequent displacement of flotsam from the underlying layer as compensation. This compensation is what is termed the "squeeze expulsion" mechanism (Savage, 1988). Because the upward flow of material that compensates percolation of jetsam may itself contain jetsam, the rate of jetsam concentration due to the segregation mechanism is represented by a nonlinear concentration gradient.

5.3 The Governing Equations for Segregation

The governing equations for mixing and segregation are derived by considering an equilibrium balance of material for the control volume (Figure 5.3). First, particles drift into the control volume by convection as a result of the bulk velocity in the active layer. The rate of jetsam dispersion into and out of the control volume may be represented, respectively, as $AuC_{J(x,y)}$ and $AuC_{J(x+\mathrm{d}x,y)}$), where A is the area normal to the bulk flow, and u is the bulk velocity. The rate of diffusional mixing is proportional to the concentration gradient and the effect of this component in the x-wise direction of the active layer may be neglected relative to the large advection term. The rate of diffusion-like mixing at each x-position in the active layer is therefore given as $-\bar{r}(\partial C_J/\partial y)$, where $\bar{r}$ is the proportionality constant equal to the product of the diffusion coefficient and the participating area in the control volume, that is, $\widetilde{D}_y A[\mathrm{s}^{-1}]$. The rate of segregation for jetsam particles is given by a nonlinear quantity, $\bar{k}C_J(1 - C_J)$ where $\bar{k}$ is the product of the area and the percolation velocity is given as $Av_p[\mathrm{m}^3\mathrm{s}^{-1}]$. By employing the Taylor series expansion, the rates of jetsam outflow from the control volume may be expressed as follows:

1. Bulk flow:

$$Au(y)C_J = Au(y)\left[C_{J|_x} + \frac{\partial}{\partial x}(C_J)\,\mathrm{d}x + \frac{\partial^2}{\partial x^2}(C_J)\,\mathrm{d}x^2 + \cdots\right] \tag{5.5}$$

2. Diffusion:

$$-\bar{r}\frac{\partial C_J}{\partial y_{|y-\mathrm{d}y,x}} = -\bar{r}\left[\frac{\partial C_J}{\partial y_{|y,x}} - \frac{\partial}{\partial y}\left(\frac{\partial C_J}{\partial y}\right)\mathrm{d}x + \cdots\right] \tag{5.6}$$

3. Segregation:

$$\bar{k}C_{\mathrm{J}|y+\mathrm{d}y,x}\left[1-C_{\mathrm{J}|y+\mathrm{d}y,x}\right]=\bar{k}\left[1-C_{\mathrm{J}|y,x}\right]\left[C_{\mathrm{J}|y,x}+\frac{\partial}{\partial y}\left(C_{\mathrm{J}}\right)\mathrm{d}y+\cdots\right] \tag{5.7a}$$

$$\bar{k}C_{\mathrm{J}|y,x}\left[1-C_{\mathrm{J}|y-\mathrm{d}y,x}\right]=\bar{k}C_{\mathrm{J}|y,x}\left[1-\left\{C_{\mathrm{J}|y,x}-\frac{\partial}{\partial y}\left(C_{\mathrm{J}}\right)\mathrm{d}y+\cdots\right\}\right] \tag{5.7b}$$

By expanding the terms given in Equations (5.5) through (5.7) and substituting the rate of jetsam inflow of particles for the control volume, the net change of jetsam concentrations becomes:

$$\widetilde{D}_y\frac{\partial^2 C_{\mathrm{J}}}{\partial y^2}\mathrm{d}x\,\mathrm{d}y\,\mathrm{d}z+\nu_{\mathrm{p}}\left(1-2C_{\mathrm{J}}\right)\frac{\partial C_{\mathrm{J}}}{\partial y}\mathrm{d}x\,\mathrm{d}y\,\mathrm{d}z=u(y)\frac{\partial C_{\mathrm{J}}}{\partial x}\mathrm{d}x\,\mathrm{d}y\,\mathrm{d}z \tag{5.8}$$

The differential equation describing the movement of jetsam concentration in the active layer may be written as:

$$\widetilde{D}_y\frac{\partial^2 C_{\mathrm{J}}}{\partial y^2}+\nu_{\mathrm{p}}\left(1-2C_{\mathrm{J}}\right)\frac{\partial C_{\mathrm{J}}}{\partial y}-u(y)\frac{\partial C_{\mathrm{J}}}{\partial x}=0 \tag{5.9}$$

In arriving at Equation (5.9), the boundary layer condition whereby $u_x \gg u_y$ has been imposed; the y-component of the species convection term has been ignored and thus the vertical movement of jetsam occurs only by percolation or diffusion.

The diffusion flux in the active layer occurs as a result of particle collision in the continuously shearing active layer. The diffusion coefficient and the bulk velocity are determined by the flow model detailed in Chapter 4. $\widetilde{D}_y$ is the kinetic diffusivity which had been computed from the granular temperature as (Savage, 1983; Hsiau and Hunt, 1993)

$$\widetilde{D}_y=\frac{d_{\mathrm{p}}\sqrt{\pi\widetilde{\widetilde{T}}}}{8\left(e_{\mathrm{p}}+1\right)\nu g_0} \tag{5.10}$$

As well, $u(y)$ is the velocity profile for the active layer which is obtained from the flow model described in Chapter 4. At this point the percolation velocity is the only remaining unknown component required to reach a solution to the segregation problem. In order to determine this velocity, the model developed by Savage (1988) for segregation in inclined chute flow might be applicable to the situation under consideration. It considers the probability for formation of a void in an underlying layer with a size sufficiently large enough to

capture the smaller particles within the overlying layer. The net percolation velocity for the smaller particles in the neighborhood might be determined as (Savage, 1988):

$$v_p = d_{ps}\left(\frac{du}{dy}\right)\frac{1}{\left(1+\overline{\eta}\,\overline{\sigma}^3\right)}\left(v_{ps}-v_{pL}\right) \tag{5.11}$$

Here the percolation velocities for smaller (jetsam), v_{ps}, and larger (flotsam) particles, v_{pL}, are given by the following equations:

$$v_{ps} = d_{pL}\left(\frac{du}{dy}\right)G\left(\overline{\eta},\overline{\sigma}\right)\left[\overline{E}-E_m+1+\frac{(1+\overline{\eta})\,\overline{\sigma}}{(1+\overline{\eta}\,\overline{\sigma})}\right]\exp\left\{\frac{(1+\bar{\eta})\,\bar{\sigma}/(1+\overline{\eta})-E_m}{\overline{E}-E_m}\right\} \tag{5.12}$$

$$v_{pL} = d_{pL}\left(\frac{du}{dy}\right)G\left(\overline{\eta},\overline{\sigma}\right)\left[\overline{E}-E_m+1+\frac{(1+\overline{\eta})}{(1+\overline{\eta}\,\overline{\sigma})}\right]\exp\left\{\frac{(1+\overline{\eta})/(1+\overline{\eta})-E_m}{\overline{E}-E_m}\right\} \tag{5.13}$$

The function $G(\overline{\eta},\overline{\sigma})$, in Equations (5.12) and (5.13), relates the packing of particles around a void to particle size ratio σ and particle number ratio, $\overline{\eta}$, and is given by the expression

$$G\left(\overline{\eta},\overline{\sigma}\right) = \frac{4k_{LT}^2\,(M/N)\,(1+\overline{\eta}\,\overline{\sigma})}{\pi\,(1+\overline{\eta})\left\{\dfrac{(1+\overline{\eta})\left(1+\overline{\eta}^2\,\overline{\sigma}^2\right)}{(1+\overline{\eta}\,\overline{\sigma})^2}+\dfrac{\overline{E}^2}{k_{AV}\,(M/N)}\right\}} \tag{5.14}$$

where $\overline{E}$ is the mean void diameter ratio and E_m is the minimum possible void diameter ratio when spontaneous percolation occurs as defined earlier. Here, M is the total number of voids in the neighborhood, N is the total number of particles in the same region, and k_{AV} is the ratio of the mean voids sphere projected area to the mean projected total area (Savage, 1988). The parameters M/N, E_m, and k_{AV} are constants that depend on particle packing, and for which appropriate values can be chosen for the particle assembly. For example, for the closest packing of spherical particles these values are: $M/N = 2$, $E_m = 0.1547$, and $k_{AV} = 0.466$ while for a simple cubic array they are, respectively, 1.0, 0.414, and 0.63 (Savage, 1988). The parameter k_{LT} in Equation (5.14) depends on the geometry of the grid chosen for the control volume and is defined as $\delta y = k_{LT}\overline{D}$ (Savage, 1988), which is the mean particle diameter in the neighborhood. The number of particles

per unit area, that is, the number density, is computed as a function of the voids area ratio, e_A, as

$$N_p = \frac{(1+\overline{\eta})}{A_s\,(1+e_A)\left(1+\overline{\eta}\,\overline{\sigma}^2\right)} \tag{5.15}$$

In the application of such a model to the rotary kiln, it must be pointed out that, as a result of jetsam segregation, the values for M/N, E_m, and k_{AV} are susceptible to changes because of rearrangement of the particle ensemble. Nevertheless, it is possible to alter these constants dynamically with respect to both time and space (e.g., for each kiln revolution or material turnover in the cross section). With the altered values of the constants the solid fraction for the segregated core may be computed with the following relationship (Savage, 1988)

$$\nu = \frac{2\,(1+\overline{\eta})\left(1+\overline{\eta}\,\overline{\sigma}^3\right)}{3k_{LT}\,(1+e_A)\left(1+\overline{\eta}\,\overline{\sigma}^2\right)\left(1+\overline{\eta}\,\overline{\sigma}\right)} \tag{5.16}$$

It should be recalled that, although a constant value of the solids concentration had been employed in the granular flow model, Equation (5.16) provides a means of determining changes in void fraction due to segregation.

5.4 Boundary Conditions

The calculation domain for jetsam segregation and the percolation process were shown in Figure 5.3. Owing to kiln rotation, an initially well mixed binary mixture will follow a specific path in the plug flow region until it crosses the yield line into the active layer. For the active layer, material enters from the plug flow region with a given jetsam concentration and then travels down the inclined plane in a streaming flow. During this journey, jetsam particles sink when the voids in the underlying layer are large enough for the particles to percolate. If this does not occur they will pass the yield line again and recirculate. The plug flow region serves only as an "escalator" and within this region particles do not mix or percolate unless small enough to undergo spontaneous percolation; a condition that is precluded from the model. The percolation process in the active layer is repeated for each material turnover, and as the jetsam content in the core increases, fines will no longer be visible at the exposed bed surface. Henein (1980) had observed that the only time fine particles are seen at the top of

the bed is when the vessel is loaded with 40–50% fines. The boundary conditions for Equation (5.9) will, therefore, depend on the operational conditions of the kiln. For a dilute mixture of jetsam particles, for example, the boundary conditions will be as follows

$$\text{at} \quad x = 0; \quad C_J = C_{J0} \tag{5.17a}$$

$$\text{at} \quad y = 0; \quad C_J = 0 \tag{5.17b}$$

$$\text{at} \quad y = \delta_x; \quad C_J(1 - C_J) = 0 \tag{5.17c}$$

where C_{J0} is the influx of jetsam particles at the apex (bed/wall boundary). Condition (5.17b) indicates that, at the free surface, there are no jetsam particles as all the fines in such a dilute mixture will percolate to the core region, whereas condition (5.17c) is the result of the nonlinear concentration term which will render pure jetsam ($C_J = 1$) at any boundary where particles are finally settled (Gibilaro and Rowe, 1974). It is assumed that this latter boundary condition can be applied at the interface between the active layer and the plug flow region, thus rendering the yield line impermeable to flotsam/jetsam percolation. Nevertheless, the percolation process described above allows particles at the interface to be replaced by those escalated by the plug flow and, as a result, the most appropriate boundary condition for the interface will be

$$\frac{\partial C_J(x, \delta_x)}{\partial y} = 0 \tag{5.17d}$$

5.5 Solution of the Segregation Equation

The basic expression describing segregation, Equation (5.9), with the appropriate boundary conditions, can be solved when the bulk velocity, the percolation velocity, and the diffusion coefficients are all determined *a priori*. The solution of the differential equation can be achieved by considering the problem in terms of several specific cases.

5.5.1 Strongly Segregating System (Case I)

For a strongly segregated binary mixture of different size particles the diffusion of jetsam particles in the vertical plane can be ignored. This situation will pertain to a very dilute mixture where $\overline{\eta} \rightarrow 0$ and from

Equation (5.4), although the gradient does not go to zero, the inference is that $C_J \to 0$. The differential equation for segregation thus becomes

$$v_p \frac{\partial C_J}{\partial y} - u_x(y) \frac{\partial C_J}{\partial x} = 0 \tag{5.18}$$

The required boundary conditions are given in Equation (5.17). It should be noted that Equation (5.18) is the same as that employed to describe segregation in chute flows. It can be solved analytically by the method of characteristics (Bridgwater, 1985; Savage, 1988). The characteristic solution would normally involve choosing a characteristic value, s, say, such that

$$\frac{dy}{ds} = v_p \tag{5.19a}$$

$$\frac{dx}{ds} = -u(y) \tag{5.19b}$$

Substituting Equation (5.19b) into (5.19a) gives

$$-u(y)\,dy = v_p dx \tag{5.19c}$$

Recalling that the velocity profile for bulk flow in the active layer was given in the flow model by the parabolic equation, that is,

$$\frac{u(y)}{u_\delta} = \kappa + a_1' \left(\frac{y}{\delta}\right) - a_2' \left(\frac{y}{\delta}\right)^2$$

This result can be substituted into Equation (5.19c), which, after integration, gives

$$\kappa y + a_1' \frac{y^2}{\delta} - a_2' \frac{y^3}{\delta^2} = -v_p x + B_1 \tag{5.19d}$$

If the integration constant B_1 is set to zero, the result is given as

$$\kappa y + \frac{a_1'}{\delta} y^2 - \frac{a_2'}{\delta^2} y^3 + v_p x = 0 \tag{5.19e}$$

The solution of Equation (5.19e) at various x-positions will yield the characteristic lines for equal jetsam concentration in the active layer.

5.5.2 Radial Mixing (Case II)

When the system contains mono-sized particles (i.e., particles are identified only by color differences) of uniform density, the percolation

term in the differential equation can be ignored and the problem reduces to that of diffusional mixing with drift. In this case, $C_J = C$ (color) and the resulting differential equation may be given by

$$\widetilde{D}_y \frac{\partial^2 C}{\partial y^2} - u_x(y) \frac{\partial C}{\partial x} = 0 \tag{5.20}$$

This is the linear diffusion problem of Graetz (Arpaci, 1966). Analytical solutions to Equation 5.20 exist for several boundary conditions. By employing the boundary condition discussed for the rotary kiln,

$$\begin{aligned} C(0, y) &= C_{J0} \\ \frac{\partial C(x, \delta_x)}{\partial y} &= 0 \\ C(x, 0) &= 0 \end{aligned} \tag{5.21}$$

The solution for the diffusional mixing may be given as (Arpaci, 1966)

$$\frac{C(x, y)}{C_{J0}} = \frac{2}{\delta_x} \sum_{n=0}^{\infty} \frac{(-1)^n}{\lambda_n} \exp\{-\lambda_n^2 x/2s\} \cos \lambda_n y \tag{5.22}$$

where, $s = u/2D$ and

$$\lambda_n = \frac{(2n+1)\pi}{2\delta_x}, \qquad n = 0, 1, 2, \ldots$$

5.5.3 Mixing and Segregation (Case III)

This is the complete solution to the mixing and segregation problem and it describes the movement of jetsam particles by the mechanism of mixing as well as segregation. The differential equation, as was given earlier, is

$$\widetilde{D}_y \frac{\partial^2 C_J}{\partial y^2} + v_p (1 - 2C_J) \frac{\partial C_J}{\partial y} - u(y) \frac{\partial C_J}{\partial x} = 0 \tag{5.23}$$

Although Equation 5.23 is nonlinear, solutions can be found by functional transformation (Ames, 1965). Analytical methods leading to the solution of the equation are presented in Appendix 5B. The

concentration of jetsam particles in the active layer is given by this solution as

$$C_{\mathrm{J}}(x,y) = \frac{1}{2}\left[1 - 2\frac{\widetilde{D}_y}{v_{\mathrm{p}}}\frac{\partial}{\partial y}\left(\ln \widetilde{Q}\right)\right] \tag{5.24}$$

where $\widetilde{Q}$ represents the solution for the special case of diffusional mixing (Case II).

5.6 Numerical Solution of the Governing Equations

In solving the governing equations by analytical methods, advantage may be taken of the symmetry of the problem as was employed in the flow model earlier in Chapter 4. Although the analytical methods suggested provide one avenue of approach to the problem, factors such as geometry preclude their ultimate exploitation for various reasons. For example, a recirculation term is required to furnish jetsam particles from the plug flow region into the active layer as was shown in Figure 5.3(a). Therefore, a finite difference numerical scheme may be easily employed. We demonstrate the development of a numerical solution of the derivative terms in the governing equations by discretizing the differential equations as follows (Anderson et al., 1984):

1. For Equation (5.18):

$$C_{i,j} = \frac{1}{\left[v_{\mathrm{p}}/\Delta y_j + u_{i-1,j}/\Delta x\right]}\left\{\frac{v_{\mathrm{p}}}{\Delta y_j}C_{i,j-1} + \frac{u_{i-1,j}}{\Delta x}C_{i-1,j}\right\} \tag{5.25}$$

2. Equation (5.20):

$$\begin{aligned} &-\left\{\frac{2\widetilde{D}_i}{\left[\Delta y_{j-1} + \Delta y_{j+1}\right]}\frac{1}{\Delta y_{j-1}} + \frac{2\widetilde{D}_i}{\left[\Delta y_{j-1} + \Delta y_{j+1}\right]}\frac{1}{\Delta y_{j+1}} + \frac{u_{i,j}}{\Delta x}\right\}C_{i,j} \\ &+\left\{\frac{2\widetilde{D}_i}{\left[\Delta y_{j-1} + \Delta y_{j+1}\right]}\frac{1}{\Delta y_{j-1}}\right\}C_{i,j-1} + \left\{\frac{2\widetilde{D}_i}{\left[\Delta y_{j-1} + \Delta y_{j+1}\right]}\frac{1}{\Delta y_{j+1}}\right\}C_{i,j+1} \\ &= -\frac{u_{i,j}}{\Delta x}C_{i+1,j} \end{aligned} \tag{5.26}$$

3. Equation (5.23) is solved numerically either by linearizing the nonlinear term and discretizing the resulting equation or by discretizing Equation (5.24) as an extension of the mixing problem. In the former case, the resulting equation is

$$C_{i,j} = \frac{1}{[2A_1 + A_2 + A_3]} \left(A_1 C_{i,j+1} + A_1 C_{i,j-1} A_3 C_{i,j-1} + A_2 C_{i-1,j} - \mathrm{d}C^2/\mathrm{d}y\right) \tag{5.27}$$

where,

$$A_1 = \widetilde{D}_i/\Delta y_j$$
$$A_2 = u_{i,j}/\Delta x$$
$$A_3 = v_{i,j}/\Delta y_j$$

The nonlinear term, $\partial C^2/\partial y$, may be discretized as

$$\frac{\partial C^2}{\partial y} = \frac{\left[C_{i,j} + C_{i,j-1}\right]^2 - \left[C_{i,j+1} + C_{i,j}\right]^2}{4\Delta y_j} + \frac{\gamma \left|C_{i,j} + C_{i,j-1}\right| \left(C_{i,j} - C_{i,j-1}\right) - \gamma \left|C_{i,j+1} + C_{i,j}\right| \left(C_{i,j+1} - C_{i,j}\right)}{4\Delta y_j} \tag{5.28}$$

As in the case of decretizing fluid flow equations, Equation (5.27) requires the appropriate "upwinding" and as a result Equation (5.28) represents the upstream donor cell difference whereby $\gamma = 1$ gives a full upstream effect. For $\gamma = 0$ the equation becomes numerically unstable (Anderson et al., 1984).

It might be noted in the preceding development that Equation (5.25) is an explicit algebraic formulation because of the parabolic nature of the differential equation. Thus, once the mixture concentration at the apex is given, the jetsam concentration along the chord length can be computed by marching down the incline. Equation (5.26) is the algebraic form of a one-dimensional diffusion/convection equation (Graetz problem) and may be solved numerically using the tri-diagonal method algorithm (TDMA; Anderson et al., 1984). Equation (5.27) is an implicit algebraic equation for the calculation of two-dimensional jetsam concentration in the cross section; it may be solved by an iterative procedure, for example, the Gauss Siedel method, whereby the nonlinear term, which is expressed

by Equation (5.28), is computed using previous values of $C_{i,j}$. In all the scenarios, a solution technique is employed whereby a set of calculations is carried out by marching down the inclined plane starting from the apex to the base. The solution of this set of calculations represents the concentration of jetsam particles for a single pass or material turnover in the cross section. Because there is no diffusion in the plug flow region, particles are allowed to drift (or recirculate) from the lower section of the plug flow/active layer interface to the upper section interface. The second set of calculations for the next pass is initiated with the convected concentration as the initial condition (boundary condition). The calculation is repeated until the overall jetsam concentration in the cross section equals the jetsam loading. Because the bed material circulates for about 3 or 4 times per each kiln revolution, this approach allows for the estimation of the number of revolutions required to accomplish complete mixing or complete segregation. The solution method, therefore, represents a pseudo-transient solution in a two-dimensional plane.

5.7 Validation of the Segregation Model

As was said earlier in the chapter, the objective of the segregation model was to determine the extent and dimensions of the segregated core and, as a result, estimate the jetsam concentration gradient. Validation of the model has been carried out against the experimental data of Henein (1980). In that work, a 40 cm I.D. drum loaded with a prescribed jetsam concentration was rotated for some desired number of times and then stopped. The bed was then sectioned using discs inserted normal to the drum axis. In each section the fines concentration was measured, beginning from the apex to the base by sieving and weighing, or by simply counting, thereby mapping out a one-dimensional representation of jetsam concentration as a function of chord length. In order to use the data we converted the two-dimensional model result into the one-dimensional representation in the experiment by averaging the jetsam concentration for all radial nodes at each x-location as

$$C_{\mathrm{J}_{x,av}} = \sum_{j=1}^{j\max} C_{\mathrm{J}_{i,j}} A_{i,j} / \sum_{j=1}^{j\max} A_{i,j} \tag{5.29}$$

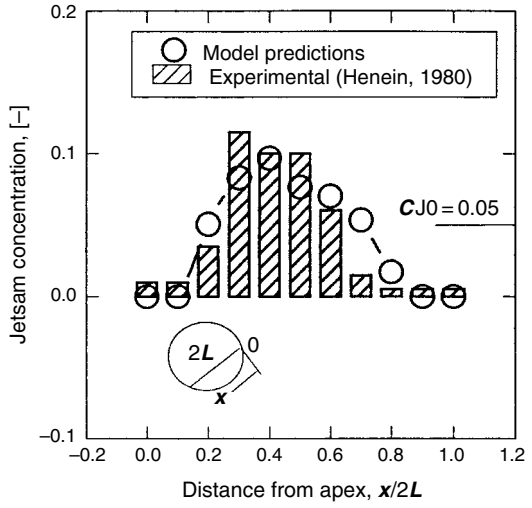

Figure 5.4 Predicted and measured profiles for jetsam concentration for a 40 cm drum: limestone, 3.11 rpm, 16% fill.

Predicted and measured radial segregation patterns determined for the case of a strongly segregated system (Case I) based on relatively low values of the jetsam loading is shown in Figure 5.4. The ratio of the fine particle diameter to the coarse particle diameter was about 0.125, which is below the threshold mark at which spontaneous percolation could occur. However, in an experiment, fines will always be sifted through the matrix of the plug flow region although this condition is precluded from the model.

5.8 Application of Segregation Model

The model has been applied for the calculation of particle concentration profiles at the mid-chord plane of a 0.41 m pilot kiln section (Figure 5.5) for which granular flow predictions were made in Chapter 4. Because Case II is for complete mixing, no further discussion on this scenario is carried out. Some results developed for the segregated core (Cases I and III) are shown in Figures 5.6 and 5.7. Notice the difference between a strongly segregated system (Case I) and combined mixing and segregation (Case III). The result shows that if diffusion is present then it will tend to spread jetsam concentration by moving fines toward the top; and when percolation ceases (Case II) the

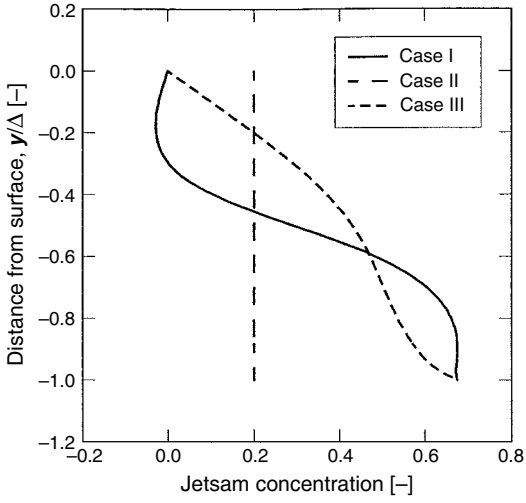

Figure 5.5 Predicted jetsam concentration in the active layer at the mid-chord position for the three cases described in the text: 0.41 m drum, 2 rpm, 12% fill, polyethylene pellets.

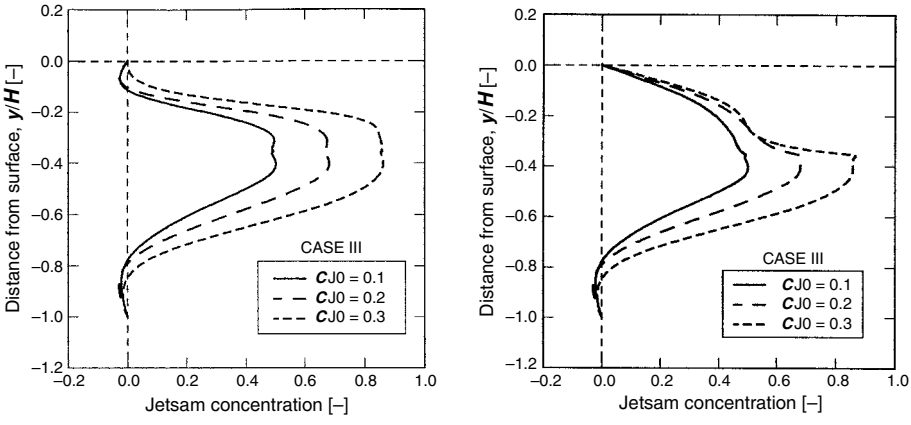

Figure 5.6 Predicted jetsam concentration in both active layer and plug flow region at mid-chord position (bed material: polyethylene; 2 rpm, 12% fill; $d_{pF}/d_{pJ} = 2$).

bed will be well mixed. For higher jetsam loading, the strongly segregated solution (Case I) is no longer applicable; rather, Case III must give a more reasonable result. Also, there is symmetry between the concentration gradient in the active layer and that in the plug flow region for Case I (Figure 5.6) due to the escalator role played by the plug flow

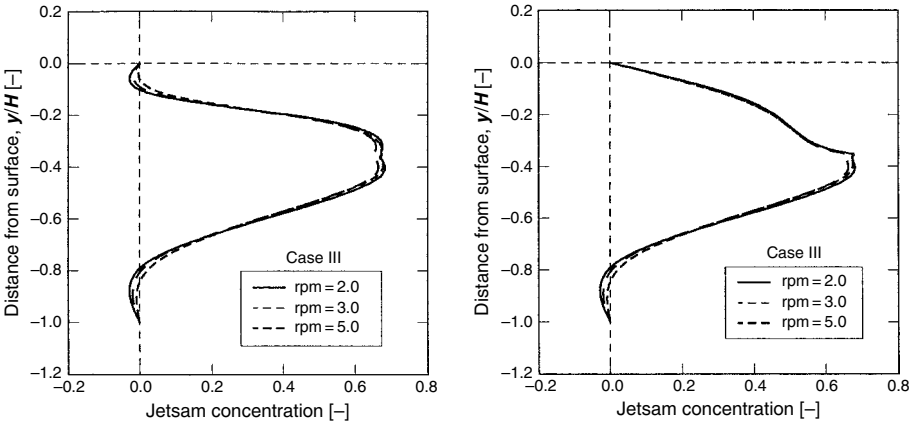

Figure 5.7 Effect of kiln speed on jetsam concentration.

region. This symmetry is distorted when Case III is employed due to the effect of the diffusion term in the governing equations, which tends to spread jetsam in the radial direction of the active layer (active layer mixing). The effect of kiln speed on segregation (Figure 5.7) indicates there is very little effect of kiln speed on the concentration profiles. This is because segregation results very rapidly and is complete by a few revolutions since, for each kiln revolution, there are 3–4 material exchanges between the plug flow and the active layer region.

The segregated tongue in a 2.5 m diameter industrial size kiln operating at 2 rpm is shown in the contour plot (Figure 5.8). The model

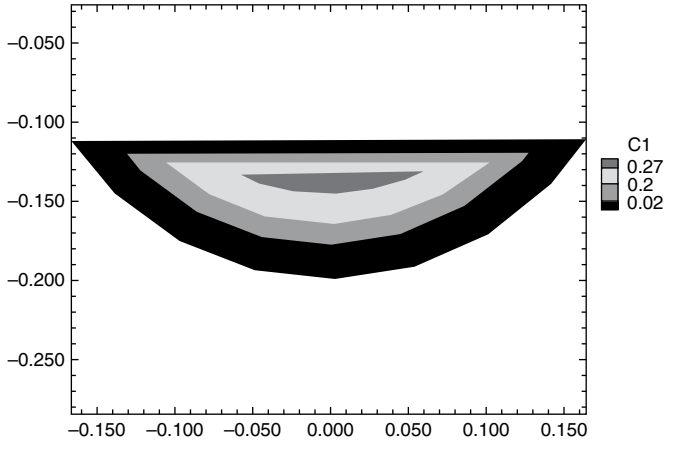

Figure 5.8 Contour plots of jetsam concentration for Case I: 0.41 m drum; 2 rpm, 12% fill; jetsam loading at 20%; polyethylene.

shows that smaller kilns tend to concentrate the fines to the center of the kiln more than larger kilns. In order words, the distribution of jetsam in a larger kiln tends to skew more to the apex, depicting a more defined segregated tongue. The reason for the difference in jetsam distribution in the two kilns may be attributed to the fact that, for the same degree of fill, the chord length in the industrial kiln is longer than that of the pilot kiln and, as a result, most of the percolation process occurs between the apex and the mid-chord.

References

M. Alonso, M. Satoh, and K. Miyanami. "Optimum combination of size ratio, density ratio and concentration to minimize free surface segregation," *Powder Technol.*, 68, 145–152, 1991.

D. A. Anderson, J. C. Tannehill, and R. H. Pletcher. *Computational Fluid Mechanics and Heat Transfer*. Hemisphere, New York, 1984.

J. Bridgwater. "Fundamental powder mixing mechanisms," *Powder Technol.*, 15, 215–236, 1976.

J. Bridgwater and N. D. Ingram. "Rate of spontaneous inter-particle percolation," *Trans. Instn. Chem. Engrs.*, 49, 163–169, 1971.

J. Bridgwater, M. H. Cooke, and A. M. Scott. "Inter-particle percolation: Equipment development and mean percolation velocities," *Trans IChemE*, 56, 157–167, 1978.

J. Bridgwater, W. S. Foo, and D. J. Stephens. "Particle mixing and segregation in failure zones—Theory and experiment," *Powder Technol.*, 41, 147–158, 1985.

L. T. Fan and R. H. Wang. "On mixing indices," *Powder Technol.*, 11, 27–32, 1975.

L. G. Gibilaro and P. N. Rowe. "A model for segregating gas fluidized bed," *Chem. Eng. Sci.*, 29, 1403–1412, 1974.

H. Henein. *Bed Behavior in Rotary Cylinders with Applications to Rotary Kilns*. PhD Dissertation, University of British Columbia, Vancouver, 1980.

H. Henein, J. K. Brimacombe, and A. P. Watkinson. "An experimental study of segregation in rotary kilns," *Met. Trans. B*, 16B, 763–774, 1985.

S. S. Hsiau and M. L. Hunt. "Shear-induced particle diffusion and longitudinal velocity fluctuations in a granular-flow mixing layer," *J. Fluid Mech.*, 251, 299–313, 1993.

N. Nityanand, B. Manley, and H. Henein (1986). "An Analysis of Radial Segregation for Different Sized Spherical Solids in Rotary Cylinders," *Met. Trans B*, 17B, 247–257.

B. L. Pollard and H. Henein. "Kinetics of radial segregation of different sized irregular particles in rotary cylinders," *Can. Met. Quart.*, 28(1), 29–40, 1989.

A. R. Rogers and J. A. Clements. "The examination of granular materials in a tumbling mixer," *Powder Technol.*, 5, 167–178, 1971.
S. B. Savage. "Granular flow down rough inclines—Review and extension." In *Mechanics of Granular Materials: New Models and Constitutive Relations* (J. T. Jenkins and M. Satake, Eds.), 261–282, Elsevier, Inc., New York, 1983.
S. B. Savage. "Symbolic computation of the flow of granular avalanches," *ASME Annual Meeting*, Chicago, 1988.
S. B. Savage and C. K. K. Lun. "Particle size segregation in inclined chute flow of dry cohesionless granular solids," *J. Fluid Mech.*, 189, 311–335, 1988.
S. B. Savage. "Granular flow materials." In *Theoretical and Applied Mechanics* (P. Germain, M. Piau, and D. Caillerie, Eds.), 241–266, Elsevier, Inc., New York, 1989.
J. C. Williams and M. I. Khan. "The mixing and segregation of particulate solids of different particle size," *The Chemical Engineer*, 269, 19–25, 1973.

Appendix 5A

Relationship Between Jetsam Loading and Number Concentration

Let the respective jetsam and flotsam loading be W_J and W_F.

$$W_J = \frac{1}{6} n_J \pi d_{pJ}^3 \rho_J \tag{5A.1}$$

$$W_F = \frac{1}{6} n_F \pi d_{pF}^3 \rho_F \tag{5A.2}$$

The jetsam concentration at kiln loading becomes

$$C_{JO} = \frac{W_J}{W_J + W_F} \tag{5A.3}$$

$$C_{JO} = \frac{\frac{1}{6} n_J \pi d_{pJ}^3 \rho_J}{\frac{1}{6} n_J \pi d_{pJ}^3 \rho_J + \frac{1}{6} n_F \pi d_{pF}^3 \rho_F} \tag{5A.4}$$

For equal density particles where $\rho_J = \rho_F$,

$$C_{JO} = \frac{n_J d_{pJ}^3}{n_J d_{pJ}^3 + n_F d_{pF}^3} \tag{5A.5}$$

By invoking a definition for number ration as $\overline{\eta} = n_G/n_F$ and $\overline{\sigma} = d_{pJ}/d_{pF}$, we have

$$C_{JO} = \frac{\overline{\eta}\,\overline{\sigma}^3}{\overline{\eta}\,\overline{\sigma}^3 + 1} \tag{5A.6}$$

Appendix 5B

Analytical Solution for CASE III Using Hopf Transformation

The differential equation for CASE III can be solved using Hopf Transformation (Ames, 1965) as follows:

$$D\frac{\partial^2 C}{\partial y^2} + \nu(1 - 2C)\frac{\partial C}{\partial y} - u\frac{\partial C}{\partial x} = 0 \tag{5B.1}$$

Let, $R(x, y) = 2C(x, y) - 1$ so that

$$\begin{aligned}
\frac{\partial R(x,y)}{\partial y} &= 2\frac{\partial C(x,y)}{\partial y} \\
\frac{\partial^2 R(x,y)}{\partial y^2} &= 2\frac{\partial^2 C(x,y)}{\partial y^2} \\
\frac{\partial R(x,y)}{\partial x} &= 2\frac{\partial C(x,y)}{\partial x}
\end{aligned} \tag{5B.2}$$

Substituting Equation (5B.2) into (5B.1) gives,

$$D\frac{\partial^2 R(x,y)}{\partial y^2} = \nu R(x,y)\frac{\partial R(x,y)}{\partial y} + u\frac{\partial R(x,y)}{\partial x} \tag{5B.3}$$

We can set $R = \partial S/\partial y$ such that

$$\begin{aligned}
\frac{\partial R}{\partial y} &= \frac{\partial^2 S}{\partial y^2} \\
\frac{\partial^2 R}{\partial y^2} &= \frac{\partial^3 S}{\partial y^3} \\
\frac{\partial R}{\partial x} &= \frac{\partial^2 S}{\partial y \partial x}
\end{aligned} \tag{5B.4}$$

Substitution of Equation (5B.4) into (5B.3) gives the Hopf transformation as

$$D\frac{\partial^3 S}{\partial y^3} = \nu\frac{\partial S}{\partial y}\cdot\frac{\partial^2 S}{\partial y^2} + u\frac{\partial^2 S}{\partial y \partial x} \tag{5B.5}$$

for which the first two terms can be rearranged as

$$\frac{\partial}{\partial y}\left[D\frac{\partial^2 S}{\partial y^2} - \frac{\nu}{2}\left(\frac{\partial S}{\partial y}\right)^2\right] = 0 \tag{5B.6}$$

We can integrate this equation by arbitrarily setting the function in x to zero to yield a solution of the differential equation as

$$D\frac{\partial^2 S}{\partial y^2} - \frac{\nu}{2}\left(\frac{\partial S}{\partial y}\right)^2 = 0 \tag{5B.7}$$

and when the function with respect to x is introduced, the original differential Equation (5B.1) becomes

$$D\frac{\partial^2 S}{\partial y^2} = \frac{\nu}{2}\left(\frac{\partial S}{\partial y}\right)^2 + u\frac{\partial S}{\partial x} \tag{5B.8}$$

It is desired to make Equation (5B.8) a linear equation of the form

$$D\frac{\partial^2 \widetilde{Q}}{\partial y^2} = u\frac{\partial \widetilde{Q}}{\partial x} \tag{5B.9}$$

where

$$\begin{aligned}
&T(x,y) = F(S(x,y))\\
&\frac{\partial T}{\partial y} = F'(S(x,y))\cdot\frac{\partial S}{\partial y}\\
&\frac{\partial T}{\partial x} = F'(S(x,y))\cdot\frac{\partial S}{\partial x}\\
&\frac{\partial^2 T}{\partial y^2} = F''(S(x,y))\frac{\partial S}{\partial y}\cdot\frac{\partial S}{\partial y} + F'(S(x,y))\frac{\partial^2 S}{\partial y^2}
\end{aligned} \tag{5B.10}$$

Substituting Equation (5B.10) into (5B.9) yields

$$D\left[F''(S)\left(\frac{\partial S}{\partial y}\right)^2 + F'(S)\frac{\partial^2 S}{\partial y^2}\right] = uF'(S)\frac{\partial S}{\partial x} \tag{5B.11}$$

Divide by $F'(S)$ for $F'(S) \neq 0$ so that

$$D\left[\frac{F''(S)}{F'(S)}\left(\frac{\partial S}{\partial y}\right)^2 + \frac{\partial^2 S}{\partial y^2}\right] = u\frac{\partial S}{\partial x} \tag{5B.12}$$

By identifying Equation (5B.12) with (5B.8) we can write

$$D\frac{F''(S)}{F'(S)} = -\frac{\nu}{2} \quad \text{or} \quad F''(S) = -\frac{\nu}{2D}F'(S)$$

which can be integrated to give

$$F(S) = A\exp(-\nu S/2D) + B \tag{5B.13}$$

Set $A = 1$ and $B = 0$ and invert it to give

$$S = -\frac{2D}{\nu}\ln\{F(S)\} = -\frac{2D}{\nu}\ln\widetilde{Q}$$

but $R = \partial S/\partial y$ so therefore

$$R(x,y) = -(2D/\nu)\frac{\partial}{\partial y}\left(\ln\widetilde{Q}\right) \tag{5B.14}$$

Substituting Equation (5B.14) into (5B.2) yields the solution for the jetsam concentration for mixing and segregation in the active layer as

$$C(x,y) = \frac{1}{2}[R(x,y) + 1]$$

that is,

$$C(x,y) = \frac{1}{2}\left[1 - \frac{2D}{\nu}\frac{\partial}{\partial y}\left(\ln\widetilde{Q}\right)\right] \tag{5B.15}$$

where $T(x,y)$ is the solution for the special case of diffusional mixing given for CASE II.